Macromolecular Research, Vol. 23, No. 8, pp 734-740 (2015)
DOI 10.1007/s13233-015-3099-9

www.springer.com/13233
pISSN 1598-5032 eISSN 2092-7673

Enhanced Biological Behavior of Bacterial Cellulose Scaffold by Creation of Macropores and Surface Immobilization of Collagen

Guangyao Xiong[1], Honglin Luo[1,2], Chen Zhang[3], Yong Zhu[4], and Yizao Wan*[,1,2]

[1]*School of Mechanical and Electrical Engineering, East China Jiaotong University, Nanchang 330013, P. R. China*
[2]*School of Materials Science and Engineering, Tianjin University, Tianjin 300072, P. R. China*
[3]*School of Optometry and Ophthalmology, Tianjin Medical University Eye Hospital, Tianjin 300384, P. R. China*
[4]*School of Chemical Engineering, Tianjin University, Tianjin 300072, P. R. China*

Received February 9, 2015; Revised May 24, 2015; Accepted May 25, 2015

Abstract: Bacterial cellulose (BC) is considered a promising three-dimensional (3D) nanofibrous scaffold for tissue engineering. To further improve its biological behavior, BC scaffold was modified by the creation of macropores and the immobilization of collagen (COL) on the surface. The creation of macropores was performed by laser perforation technique and the immobilization of collagen was achieved by solution immersion and subsequent crosslinking. The as-prepared macroporous BC/COL nanocomposite (denoted as mBC/COL) was characterized by SEM, FTIR, contact angle measurement, and dynamic mechanical analysis, and its cell behavior was evaluated by MTT assay. SEM and FTIR confirmed the presence of collagen coating and patterned macropores (300 μm). Although the presence of macropores and collagen reduced its storage modulus and hydrophilicity, mBC/COL exhibited sufficient stiffness and wettability. More importantly, preliminary cell studies demonstrated that mBC/COL exhibited improved biological activity over BC and BC/COL due to the co-existence of macropores and collagen.

Keywords: bacterial cellulose, collagen, macropore, cell behavior, tissue engineering scaffold.

Introduction

Recently, bacterial cellulose (BC) has received tremendous interest due to its numerous favorable characteristics. BC is synthesized extracellularly by the bacterium *Acetobacter xylinum*. It exhibits high water holding capacity and porosity, high crystallinity and polymerization, high tensile strength and modulus (the effective modulus of single fibrils of BC ranges from 79 to 88 GPa versus 29 to 36 GPa for plant cellulose[1]), fine web-like network, and good biocompatibility.[2,3] More importantly, it has a nano-sized fiber diameter, microscopically similar to collagen nanofibers in natural tissues.[4,5] All these unique properties make it a promising collagen-mimicking nano-component in tissue engineering.[5-7] However, despite these advantages, some drawbacks impede the usage of BC in biomedical field. Two of the biggest problems are the absence of macropores (defined in the literature as pores with a diameter ≥100 μm[8,9]) within the BC scaffold[10] and its low biological activity as a polysaccharide compared to proteins.[11] Therefore, engineering porosity in the BC scaffold and coating or hybridizing BC with bioactive components are of prime importance in developing BC-based scaffolds.

It has been well documented that pore structure is an essential consideration in the development of scaffolds for tissue engineering. Pores must be interconnected and large enough to allow for cell growth, migration and nutrient flow, new tissue formation and remodeling so as to facilitate host tissue integration upon implantation.[9] Although the optimal scaffold pore size is still debatable, it is generally agreed that the lower limit of pore size is 100 μm,[12] which is not present in the pristine BC scaffold.[13] As a result, numerous approaches have been developed to create macropores in BC scaffolds including adding paraffin wax microspheres in the culture medium of BC,[14] or placing cylindrical porogens into the early synthesized BC pellicles.[15] Compared with those mechanical methods, creating macropores in a BC scaffold by laser perforation technique shows some advantages[13,16,17] including controllable pore size and shape.

In order to render BC with sufficient biological activity, different bioactive materials such as collagen,[18,19] gelatin,[20-22] polylysine,[11] chitosan,[23,24] heparin,[25,26] and even bone morphogenetic protein-2 (BMP-2)[3] have been coated on or hybridized with BC by using methods such as "*in situ* biosynthesis"[27,28] or "post solution immersion".[11,22,24-26] The former is to add bioactive materials or even graphene[29] and graphene oxide[30] into the culture medium of BC and the latter is to immerse BC (usually in the hydrated state) in the solution of bioactive materials. In our previous studies, we modified BC with

*Corresponding Author. E-mail: yzwantju@126.com

collagen using the *in situ* biosynthesis method.[18] We chose collagen because it is one of the major components of extracellular matrix (ECM) and exhibits many attractive properties, including low immunogenicity, excellent biocompatibility and biodegradability, which can enhance tissue regeneration and promote cellular adhesion, growth and proliferation.[31] The *in situ* biosynthesis process was simple and green but the control of collagen content in the BC/collagen composites was not easy.

Despite the advances in engineering porosity and surface bioactivity of BC, there is no report addressing the dual modifications of BC by creating macropores in BC scaffolds and immobilizing bioactive components on the surface of BC nanofibers.

Herein, for the first time, BC was modified by simultaneous creation of macropores and surface immobilization of collagen. The BC scaffold with patterned macropores (denoted as mBC/COL hereinafter) was fabricated by an infrared laser perforate technique. Then, collagen was immobilized on BC by solution immersion method such that its content on BC can be accurately adjusted by changing the concentration of collagen solution and immersion time. In addition, in order to increase the adhesion of collagen on BC, crosslinking with procyanidin (PA) was performed considering PA was shown to be effective for the crosslinking of gelatin on BC without cytotoxicity.[20] The resultant mBC/COL nanocomposite scaffold was characterized by SEM, FTIR, and DMA. Moreover, MDA-MB-231 and MCF-7 cell lines were selected to determine the cytocompatibility of the mBC/COL scaffold.

Experimental

Preparation of BC Pellicles. The preparation and purification procedures of BC pellicles were described previously.[32,33] Briefly, the bacterial strain, *Acetobacter xylinum* X-2, was grown in the culture media containing 0.3 wt% green tea powder (analytical grade) and 5 wt% sucrose (analytical grade) for 7 days. The pH of the medium was adjusted to 4.5 by acetic acid. BC pellicles were purified by soaking in deionized water at 90 ºC for 2 h followed by boiling in a 0.5 M NaOH solution for 15 min. The BC pellicles with a diameter of 90 mm were then washed with deionized water several times and soaked in 1% NaOH for 2 days. Finally, the BC pellicles were washed free of alkali.

Creation of Macropores in BC Scaffold. Macropores in BC hydrogel were created by using infrared laser following the previously reported process.[13] Briefly, the pore pattern (including distance between neighboring pores and pore diameter) was initially designed by a commercial CAD software and input to a computer. The BC hydrogels with a thickness of 5 mm were then perforated using a CO_2 excimer laser (wavelength 10.6 μm) according to the designed pattern to obtain a BC scaffold with patterned macropores (named as mBC hereinafter). In this work, the designed pore size and pore distance were 300 and 1,000 μm, respectively, since a pore size of ~300 μm is favorable for bone formation and vascularization.[34-36]

Immobilization of Collagen on mBC Nanofibers. The immobilization of collagen on mBC nanofibers was carried out by solution immersion method. In a typical process, mBC and BC (as a control) hydrogels were immersed in an optimized collagen solution (0.075 wt%) under constant agitation in a shaker for 30 h at 37 ºC. Afterwards, crosslinking of these samples was performed by immersion in PBS solution containing 0.5 wt% PA under constant shaking for 2 h at 37 ºC and followed by thoroughly washing with deionized water, thus obtaining mBC/COL and BC/COL nanocomposites.

Characterization of mBC/COL Nanocomposite. The morphology of lyophilized scaffolds (BC, BC/COL, and mBC/Col) was observed by using a Nano 430 field emission scanning electron microscope (FE-SEM), FEI, USA. For FE-SEM observations, samples were sputter coated with gold at 10 mA for 3 min and were observed at an accelerating voltage of 10 kV.

The lyophilized BC, BC/COL, and mBC/COL samples were subjected to FT-IR analysis. The spectra were recorded by Shimadzu IRPrestige-21 (Japan) in a transmittance mode. FTIR spectra were recorded in a spectral range of 4000-400 cm^{-1} with a resolution of 4 cm^{-1}.

Similar to our previous work,[13] the porosity of various scaffolds were determined by a PoreMaster 60 GT mercury intrusion porosimeter (Quantachrome) that could measure pore diameter ranging from 950 μm up to 3.6 nm.

Contact angle measurement was conducted using the sessile drop method on a DropMaster 300 liquid/solid interface analyzer (Japan) equipped with a CCD camera using deionized water as the medium at room temperature. A microliter water droplet was dropped onto the surfaces of air-dried samples at room temperature and the contact angle was measured 10 s afterwards. The captured images of sessile drops were analyzed using drop-shape analysis SCA20 software. All contact angles were determined by averaging values measured at five different points on each sample surface.

Dynamic mechanical properties of various samples in the wet state were examined using dynamic mechanical analysis (DMA). DMA was performed from -50 to 100 ºC at a heating rate of 2 ºC/min under nitrogen atmosphere by using a DMA Q800 (TA Instruments, USA) analyzer. The single cantilever mode at a strain frequency of 1 Hz and amplitude of 15 μm was used during testing.

Cell Studies. Breast cancer cells including MDA-MB-231 and MCF-7 cell lines, supplied by Tianjin Medical University Cancer Institute and Hospital, Tianjin, China, were used for preliminary cell studies. Cells were cultured in Dulbecco's modified Eagle's medium (DMEM, Gibcol, USA) containing 10% fetal bovine serum (FBS) and 1% penicillin-streptomycin. The medium was replaced every 3 days and cultures were maintained at 37 ºC in a humidified 5% CO_2 incubator. After reaching 80% confluence, the cells were harvested by tryp-

sin/EDTA treatment and counted with a hemocytometer.

The cell proliferation was evaluated by the colorimetric MTT assay. First, cells were maintained in DMEM (Gibco) with 10% FBS (Gibco) at 37 ºC in a 5% CO_2 incubator. Monolayer cells were harvested by trypsin/EDTA (ethylenediaminetetraacetic acid) treatment. Before cell seeding, circular BC specimens (Φ10 × 1 mm) were sterilized with UV radiation. After sterilization, the scaffolds were pre-soaked in DMEM for at least 12 h. Subsequently, the scaffolds were incubated in 6-well tissue culture plates with cells for 1, 3, 5, and 7 days at 37 ºC in a 5% CO_2 incubator at a density of 2×10^5 cell/mL. After incubation, the cell-scaffold constructs were rinsed with PBS to remove non-adhering cells, followed by incubation in the culture medium (2 mL) containing 200 μL MTT reagent for 4 h under the same conditions as described above. After removal of the medium, 1 mL of DMSO was added to the wells to dissolve the converted dye. The solution (150 μL) from each sample was transferred to 96-well plates and the optical density (O.D.) was measured with a plate reader at an absorbance of 490 nm.

Statistical Analysis. All experiments were performed in triplicate unless otherwise stated. Statistical analysis of data was performed using an SPSS system. All data were presented as mean values ± standard deviation (SD). Results with *p*-values of <0.05 were considered statistically significant.

Results and Discussion

Morphology. As there are no obvious differences in the macro-photos and low magnification SEM images among pristine BC, BC/COL, and mBC/COL, Figure 1 shows representative photographs of pristine BC. Figure 1(a) reveals that aligned channels were created in the BC scaffold by computer-aided laser perforation technique. As displayed in Figure 1(b), the obtained pore diameter is about 300 μm and the spacing between neighbor pores is *ca*. 970 μm for BC, which are close to the intended values. BC/COL and mBC/COL show the same patterns (not shown). Figure 1(c) demonstrates that the wall of each macropore is porous, consisting of nanofibers and micropores.

As shown in Figure 2(a)-(c), after immersion in collagen solution and crosslinking by PA, the semi-transparent white BC pellicle becomes reddish-brown BC/COL and mBC/COL. It is found that the color of mBC/COL (Figure 2(c)) is slightly

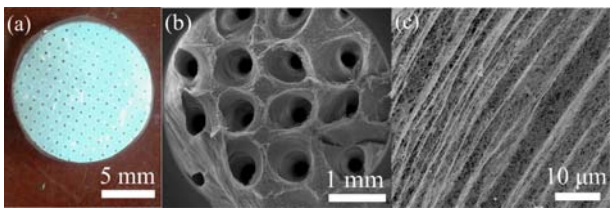

Figure 1. A photograph (a) and SEM images of BC with patterned macropores (b) and the walls of macropores (c).

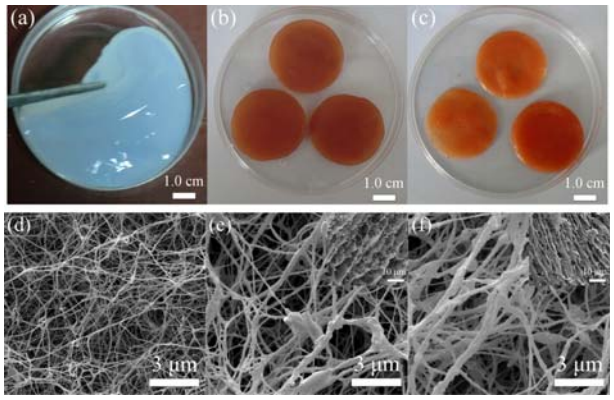

Figure 2. Photographs (a-c) and SEM images (d-f) of BC (a and d), BC/COL (b and e), and mBC/COL (c and f) (insets showing corresponding cross-sectional images).

deeper than that of BC/COL (Figure 2(b)). This color difference is due to the presence of macropores in mBC/COL which not only increase the contact area between BC and collagen solution but also promote the diffusion of collagen molecules into the interior of BC pellicles, thus resulting in more uniform immobilization of collagen molecules on mBC as compared to BC. The difference in immobilized collagen can also be proved by high magnification SEM images (Figure 2(d)-(f)). The BC image (Figure 2(d)) clearly shows a typical 3D interconnected porous structure. In the case of BC/COL and mBC/COL, the nanofibers become thicker due to the immobilization of collagen. Occasionally, collagen clots are observed. A comparison between Figure 2(e) and Figure 2(f) reveals that collagen is more evenly immobilized on mBC compared to BC, which is consistent with the color change. The cross-sectional images (insets in Figure 2(e) and (f)) of BC/COL and mBC/COL show layered structure consisting of collagen-covered fibers, which is similar to that reported by Saska *et al.*[19] Porosity measurement (Figure 3) reveals that collagen coating sig-

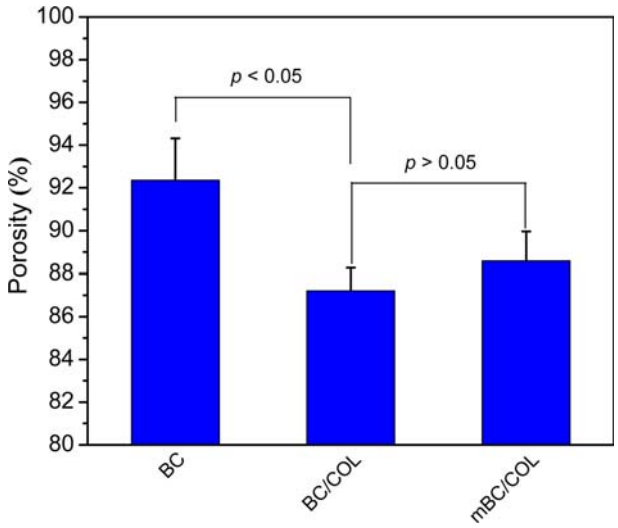

Figure 3. The overall porosity of BC, BC/COL, and mBC/COL.

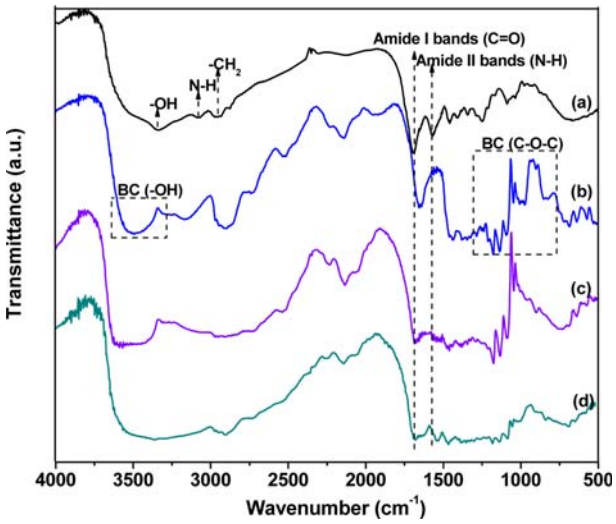

Figure 4. FTIR spectra of collagen (a), BC (b), BC/COL (c), and mBC/COL (d).

nificantly reduces the overall porosity of BC scaffold (p<0.05). However, the creation of macropores does not significantly increase the porosity of the BC/COL scaffold (p>0.05).

FTIR Results. Figure 4 shows the FTIR spectra of collagen, BC, BC/COL, and mBC/COL. Typical IR bands for pure collagen are observed in Figure 4(a): O-H stretching at 3430 cm^{-1}, N-H stretching at ~3060 cm^{-1}, -CH_2 asymmetric stretching at ~2900 cm^{-1}, C=O stretching at 1650 cm^{-1} for the amide I, and N-H deformation at 1545 cm^{-1} for the amide II.[19] Figure 4(b) shows typical IR bands for BC: 3300-3100 cm^{-1} and 1250-850 cm^{-1} correspond to -OH and C-O-C peaks of BC, respectively, which is consistent with that observed by other research groups.[37] As can be seen from Figure 4(c) and (d), for BC/COL and mBC/COL, the peak corresponding to the amide I of collagen is observed, indicating the presence of collagen in the cellulose network.

Mechanism on Immobilization of Collagen on BC Nanofibers. Figure 5 illustrates the schematic diagram of the immobilization of collagen molecules on BC nanofibers. In solution, the peptide amide bond (-CO-NH-) may experience electron rearrangement to produce O^- and N^+. Since BC surface was negatively charged, collagen molecules can be adsorbed onto BC nanofiber surfaces *via* electrostatic attraction and enwrap BC nanofibers. The attraction is unstable and the collagen molecules will be desorbed from the surface of BC nanofibers in subsequent cleaning and soaking. Upon crosslinking with PA, the crosslinked collagen on BC surface can stay in place even after intensive cleaning. This is due to the fact that crosslinked collagen on BC, like a continuous shell that enwraps BC as illustrated in Figure 5, is more stable in comparison to the uncrosslinked one. Therefore, crosslinking with PA can ensure stable collagen immobilization on BC nanofibers.

Wettability. Wettability is a crucial parameter for scaffold materials when used in tissue engineering. BC is a highly

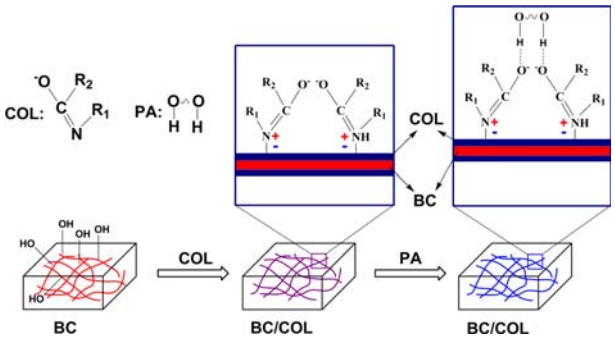

Figure 5. Mechanism of immobilization of collagen on BC nanofibers.

Table I. Water Contact Angle of BC, BC/COL, and mBC-COL

Sample	Contact Angle (°)	SD
BC	50.0	2.4
BC/COL	75.1	2.8
mBC/COL	76.3	1.9

hydrophilic material due to the existence of a large amount of surface hydroxyl groups. Therefore, it is hypothesized that the hydrophilicity will decrease when collagen molecules are immobilized and crosslinked with PA which decreases the amount of surface hydroxyl groups. In order to test the hypothesis, the contact angle of BC, BC/COL, and mBC/COL was measured. The water contact angle for BC, BC/COL, and mBC/COL is summarized in Table I. Notably, the static water contact angle of BC/COL (75.1 ± 2.8°) and mBC/COL (76.3 ± 1.9°) is significantly higher than that (50.0 ± 2.4°) of BC (p < 0.01 in both cases). This demonstrates that the immobilization of collagen significantly decreases the wettability of BC. The decrease in surface hydrophilicity is attributed to the decreased amount of hydroxyl groups on BC nanofibers. A similar increase in contact angle of BC was reported by Saska *et al*. when collagen was incorporated in BC network.[19] Note that the difference in contact angle between mBC/COL and BC/COL is not significant (p>0.05), indicating that the existence of macropores in mBC/COL exerts no effect on the hydrophilicity of BC/COL.

Dynamic Mechanical Analysis. Understanding the variations in mechanical properties with changes of loading frequency is important in tissue engineering as native tissues constantly experience changes in mechanical loading.[38] Therefore, DMA was used to compare the viscoelastic properties of BC, BC/COL, and mBC/COL. Figure 6 shows the storage modulus of these materials at constant temperature, which represents the stiffness of a viscoelastic material and shows the amount of energy stored in it. Note that all three materials do not exhibit large variations in storage modulus with the changing loading frequency except for the initial stage at a frequency of <0.1 Hz. As expected, by immobilizing colla-

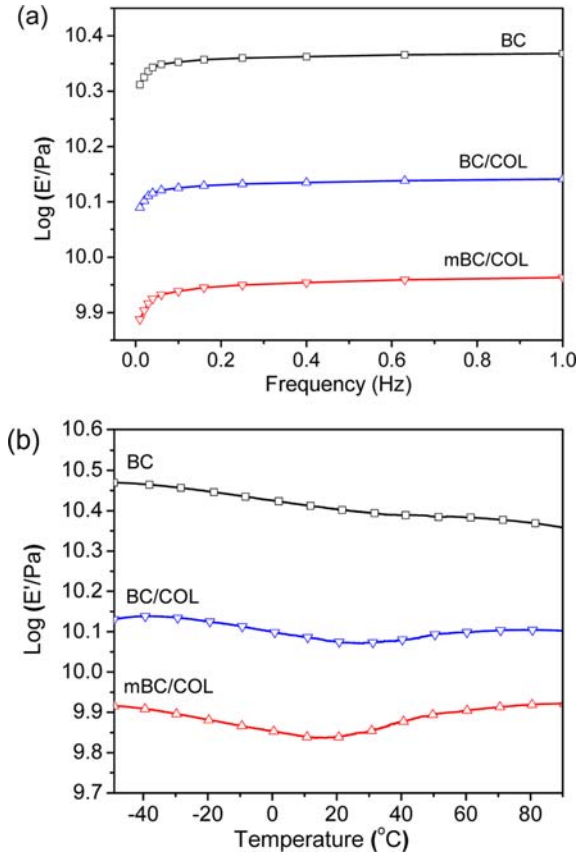

Figure 6. Storage modulus of BC, BC/COL, and mBC/COL as a function of frequency (a) and temperature (b).

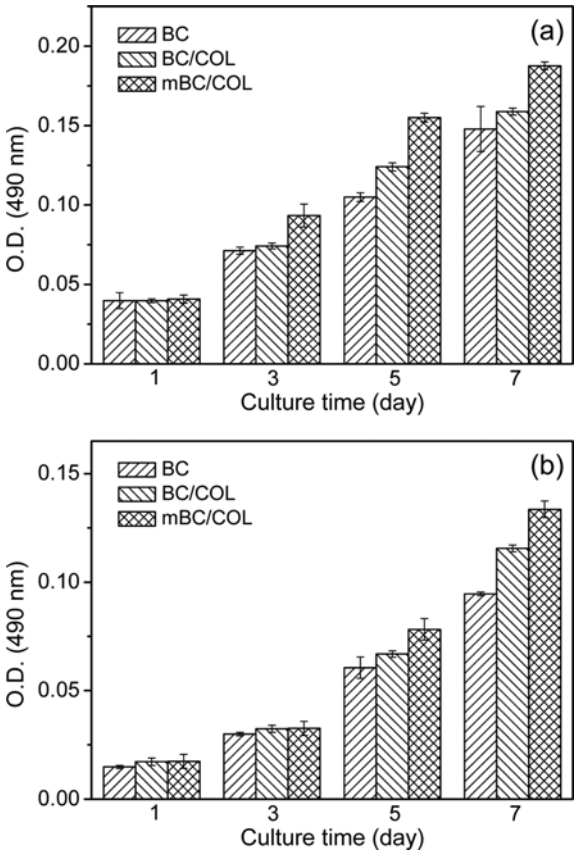

Figure 7. MTT assay for proliferation of MDA-MB-231 (a) and MCF-7 (b) cell lines cultured on BC, BC/COL, and mBC/COL.

gen on BC, the storage modulus decreases. This suggests that the existence of collagen in the BC network decreases the mechanical properties of pristine BC, which is consistent with previous results conducted by static mechanical testing.[19] Further decrease in storage modulus is detected when macropores are created in mBC/COL. A similar reduction in tensile strength was observed when macropores were created in BC.[13] Figure 6(b) compares the storage modulus of BC, BC/COL, and mBC/COL at constant frequency. The same trend is observed, namely, the value of storage modulus follows the same order of BC>BC/COL>mBC/COL. In addition, the variation of storage modulus is minimal over a temperature range of -40 to 80 ºC, indicating that the three materials have relatively stable mechanical properties. Previous studies showed that collagen scaffold exhibited a storage modulus of about 10 MPa[39] and poly(*D,L*-lactide-*co*-glycolide) (PLGA)/nano-hydroxyapatite composite scaffolds had a storage modulus of 724 MPa.[40] The highest storage modulus of a corn starch/poly(vinylidene fluoride) blend was 2,000 MPa at 37 ºC.[41] Therefore, we believe that, while laser perforation leads to a 45% decrease in storage modulus as compared to BC/COL, the storage modulus of mBC/COL (~7,000 MPa) is sufficient as a tissue engineering scaffold.

Cell Behavior. The ability to promote the proliferation of cells is one of the most important aspects of a scaffold. To quantitatively compare such characteristics, both MDA-MB-231 and MCF-7 cells were cultured on BC, BC/COL, and mBC/COL scaffolds for various culture times. The results are shown in Figure 7. The Figure shows O.D. value (an indication of cell viability), of the attached cells on these scaffolds after the cells were cultured for 1, 3, 5, and 7 days. The MTT assay results demonstrate that, for each scaffold, the viability of the proliferated cells increases with increasing cell culture time. The viability of both MDA-MB-231 and MCF-7 cells on BC steadily increases, indicating robust proliferation on the biocompatible BC. Note that BC/COL shows a significantly higher viability at day 3, 5, and 7 for MDA-MB-231 and at day 5 and 7 for MCF-7 in comparison to pristine BC (p<0.05) even though BC/COL has a significantly lower porosity. This improved cell viability is due to the fact that collagen is the dominant organic matrix in human bones and thus can produce a biomimetic extracellular environment for cell attachment and proliferation. A similar result was also reported by Cai and Yang.[42] Interestingly, at day 3, 5, and 7 for MDA-MB-231 and at day 5 and 7 for MCF-7, the O.D. value of mBC/COL is significantly higher than that of BC/COL although

their porosity is not significantly different. This finding suggests that the presence of patterned macropores in BC/COL greatly improves the proliferation of cells, which is consistent with previous results. For instance, our previous work indicated that the BC/gelatin/hydroxyapatite scaffolds with patterned macropores promoted the attachment and proliferation of chondrogenic rat cells.[16] Martinez-Ramos *et al.* found that the acrylate copolymers-based scaffolds with aligned channels achieved a uniform colonization by neural cells.[43] A very recent study demonstrated that perforated pores (with the size of 100 μm) facilitated permeability and vessel ingrowth and thus promoted axon extension since the perforated pores could ensure sufficient vascular supply from surrounding tissues.[44]

It should be noted that the *in vitro* results are very preliminary and further evaluation regarding the biocompatibility of these materials is required. Moreover, the optimization of pore size and distance is also necessary to target different types of cells. However, the results we reported here indicate that the dual modifications of the creating macropores and immobilizing collagen can significantly enhance the cell viability of the BC scaffold.

Conclusions

The BC scaffold was modified by both creating patterned macropores and immobilizing collagen on BC nanofibers. An mBC/COL nanocomposite scaffold with patterned macropore (around 300 μm in diameter) and immobilized collagen was produced by laser perforation technique and solution immersion. Chemical crosslinking with PA was used to ensure strong collagen-BC adhesion. The patterned macropores and collagen coating were confirmed by SEM observation and the existence of collagen in BC network was evidenced by FTIR analysis. Contact angle measurement revealed that the immobilization of collagen decreased the hydrophilicity of BC. DMA analysis confirmed that both immobilization of collagen and creation of macropores decreased the storage modulus of BC. In spite of the reduction, the storage modulus of mBC/COL is still sufficient as a tissue engineering scaffold. Cell studies suggested that, while BC and BC/COL scaffolds supported the proliferation of MDA-MB-231 and MCF-7 cells, the mBC/COL scaffold with dual modifications (macropores and collagen) showed the highest cell viability among the three scaffolds. These findings indicated that simultaneous creation of macropores within BC scaffold and surface immobilization of collagen on BC nanofibers can greatly improve the biological activity of BC scaffold. The findings presented in this study may offer a new paradigm for the design of BC-based scaffolds with improved biological performance.

Acknowledgments. This work is supported by the National Natural Science Foundation of China (Grants No. 51172158 and 81200663) and the Science & Research Foundation of Jiangxi Province (Grant No. 20151BDH80061).

References

(1) S. Tanpichai, F. Quero, M. Nogi, H. Yano, R. J. Young, T. Lindstrom, W. W. Sampson, and S. J. Eichhorn, *Biomacromolecules*, **13**, 1340 (2012).
(2) R. A. N. Pertile, S. Moreira, R. M. Gil da Costa, A. Correia, L. Guardao, F. Gartner, M. Vilanova, and M. Gama, *J. Biomater. Sci. Polym. Ed.*, **23**, 1339 (2012).
(3) S. Saska, R. M. Scarel-Caminaga, L. N. Teixeira, L. P. Franchi, R. A. Dos Santos, A. M. M. Gaspar, P. T. de Oliveira, A. L. Rosa, C. S. Takahashi, Y. Messaddeq, S. J. L. Ribeiro, and R. Marchetto, *J. Mater. Sci. Mater. Med.*, **23**, 2253 (2012).
(4) H. Bäckdahl, G. Helenius, A. Bodin, U. Nannmark, B. R. Johansson, B. Risberg, and P. Gatenholm, *Biomaterials*, **27**, 2141 (2006).
(5) H. Bäckdahl, M. Esguerra, D. Delbro, B. Risberg, and P. Gatenholm, *J. Tissue Eng. Regen. Med.*, **2**, 320 (2008).
(6) K. A. Zimmermann, J. M. LeBlanc, K. T. Sheets, R. W. Fox, and P. Gatenholm, *Mater. Sci. Eng. C*, **31**, 43 (2011).
(7) W. K. Czaja, D. J. Young, M. Kawecki, and R. M. Brown, Jr., *Biomacromolecules*, **8**, 1 (2007).
(8) J. C. Le Huec, T. Schaeverbeke, D. Clement, J. Faber, and A. Le Rebeller, *Biomaterials*, **16**, 113 (1995).
(9) J. M. Taboas, R. D. Maddox, P. H. Krebsbach, and S. J. Hollister, *Biomaterials*, **24**, 181 (2003).
(10) C. Gao, Y. Wan, C. Yang, K. Dai, T. Tang, H. Luo, and J. Wang, *J. Porous. Mater.*, **18**, 139 (2011).
(11) C. Gao, Y. Wan, X. Lei, J. Qu, T. Yan, and K. Dai, *Cellulose*, **18**, 1555 (2011).
(12) H. J. Kim, U.-J. Kim, G. G. Leisk, C. Bayan, I. Georgakoudi, and D. L. Kaplan, *Macromol. Biosci.*, **7**, 643 (2007).
(13) G. Xiong, H. Luo, F. Gu, J. Zhang, D. Hu, and Y. Wan, *J. Biomater. Nanobiotechnol.*, **4**, 316 (2013).
(14) M. Zaborowska, A. Bodin, H. Backdahl, J. Popp, A. Goldstein, and P. Gatenholm, *Acta Biomater.*, **6**, 2540 (2010).
(15) H. Martinez, C. Brackmann, A. Enejder, and P. Gatenholm, *J. Biomed. Mater. Res. Part A*, **100A**, 948 (2012).
(16) J. Wang, C. Yang, Y. Wan, H. Luo, F. He, K. Dai, and Y. Huang, *Soft Mater.*, **11**, 173 (2013).
(17) H. Ahrem, D. Pretzel, M. Endres, D. Conrad, J. Courseau, H. Mueller, R. Jaeger, C. Kaps, D. O. Klemm, and R. W. Kinne, *Acta Biomater.*, **10**, 1341 (2014).
(18) H. Luo, G. Xiong, Y. Huang, F. He, Y. Wang, and Y. Wan, *Mater. Chem. Phys.*, **110**, 193 (2008).
(19) S. Saska, L. N. Teixeira, P. T. de Oliveira, A. M. M. Gaspar, S. J. Lima Ribeiro, Y. Messaddeq, and R. Marchetto, *J. Mater. Chem.*, **22**, 22102 (2012).
(20) J. Wang, Y. Z. Wan, H. L. Luo, C. Gao, and Y. Huang, *Mater. Sci. Eng. C*, **32**, 536 (2012).
(21) J. Wang, Y. Wan, J. Han, X. Lei, T. Yan, and C. Gao, *Micro Nano Lett.*, **6**, 133 (2011).
(22) S.-T. Chang, L.-C. Chen, S.-B. Lin, and H.-H. Chen, *Food Hydrocoll.*, **27**, 137 (2012).
(23) W.-C. Lin, C.-C. Lien, H.-J. Yeh, C.-M. Yu, and S.-H. Hsu, *Carbohydr. Polym.*, **94**, 603 (2013).
(24) V. Dubey, L. K. Pandey, and C. Saxena, *J. Membr. Sci.*, **251**, 131

(2005).
(25) J. Wang, Y. Wan, and Y. Huang, *IET Nanobiotech*, **6**, 52 (2012).
(26) Y. Wan, C. Gao, M. Han, H. Liang, K. Ren, Y. Wang, and H. Luo, *Polym. Adv. Technol.*, **22**, 2643 (2011).
(27) S. Taokaew, S. Seetabhawang, P. Siripong, and M. Phisalaphong, *Materials*, **6**, 782 (2013).
(28) M. Phisalaphong and N. Jatupaiboon, *Carbohydr. Polym.*, **74**, 482 (2008).
(29) J. Jin, G. Zuo, G. Xiong, H. Luo, Q. Li, C. Ma, D. Li, F. Gu, Y. Ma, and Y. Wan, *J. Mater. Sci. Mater. Med.*, **25**, 1025 (2014).
(30) H. Si, H. Luo, G. Xiong, Z. Yang, S. R. Raman, R. Guo, and Y. Wan, *Macromol. Rapid Commun*., **35**, 1706 (2014).
(31) A. M. Ferreira, P. Gentile, V. Chiono, and G. Ciardelli, *Acta Biomater.*, **8**, 3191 (2012).
(32) L. Hong, Y. L. Wang, S. R. Jia, Y. Huang, C. Gao, and Y. Z. Wan, *Mater. Lett*., **60**, 1710 (2006).
(33) Y. Z. Wan, L. Hong, S. R. Jia, Y. Huang, Y. Zhu, Y. L. Wang, and H. J. Jiang, *Compos. Sci. Technol.*, **66**, 1825 (2006).
(34) V. Karageorgiou and D. Kaplan, *Biomaterials*, **26**, 5474 (2005).
(35) E. Tsuruga, H. Takita, H. Itoh, Y. Wakisaka, and Y. Kuboki, *J. Biochem.*, **121**, 317 (1997).
(36) H. E. Gotz, M. Muller, A. Emmel, U. Holzwarth, R. G. Erben, and R. Stangl, *Biomaterials*, **25**, 4057 (2004).
(37) C. J. Grande, F. G. Torres, C. M. Gomez, O. P. Troncoso, J. Canet-Ferrer, and J. Martínez-Pastor, *Mater. Sci. Eng. C*, **29**, 1098 (2009).
(38) C. Schindler, B. L. Williams, H. N. Patel, V. Thomas, and D. R. Dean, *Polymer*, **54**, 6824 (2013).
(39) K. Pietrucha, *Int. J. Biol. Macromol.*, **36**, 299 (2005).
(40) M. V. Jose, V. Thomas, K. T. Johnson, D. R. Dean, and E. Nyairo, *Acta Biomater.*, **5**, 305 (2009).
(41) J. D. A. S. Pereira, R. C. T. Camargo, J. C. S. C. Filho, N. Alves, M. A. Rodriguez-Perez, and C. J. L. Constantino, *Mater. Sci. Eng. C*, **36**, 226 (2014).
(42) Z. Cai and G. Yang, *J. Appl. Polym. Sci.*, **120**, 2938 (2011).
(43) C. Martinez-Ramos, A. Valles-Lluch, J. M. G. Verdugo, J. L. G. Ribelles, J. A. Barcia, A. B. Orts, J. M. S. Lopez, and M. M. Pradas, *J. Biomed. Mater. Res. A*, **100A**, 3276 (2012).
(44) Y. Fukuda, W. Wang, S. Ichinose, H. Katakura, T. Mukai, and K. Takakuda, *J. Biomed. Mater. Res. A*, **102**, 674 (2014).